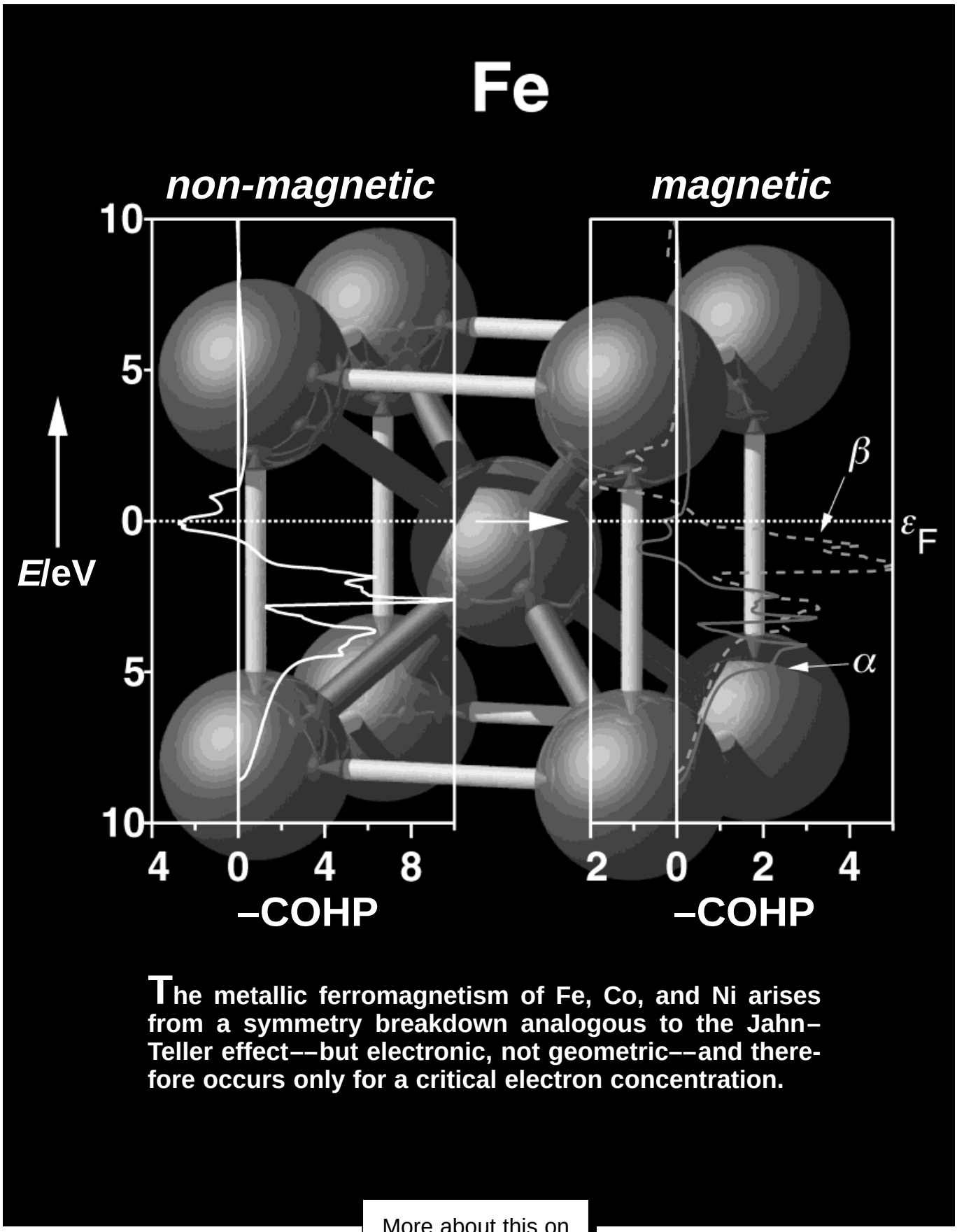

The metallic ferromagnetism of Fe, Co, and Ni arises from a symmetry breakdown analogous to the Jahn–Teller effect––but electronic, not geometric––and therefore occurs only for a critical electron concentration.

More about this on the following pages

  1433-7851/99/3810-1389 $ 17.50+.50/0

Ferromagnetism in Transition Metals: A Chemical Bonding Approach**

Gregory A. Landrum and Richard Dronskowski*

In memory of Jean Rouxel

While the microscopic factors underlying molecular magnetism are reasonably well understood from a chemical point of view, the same cannot be said of collective magnetic phenomena such as ferromagnetism and antiferromagnetism. Herein we present a simple and accurate explanation, extracted from the results of band structure calculations based on first principles, for the appearance of ferromagnetism in iron, cobalt, and nickel. The search for an understanding of ferromagnetism is truly historical: early explanatory attempts date back to the 1920s and 1930s,[1] and the first reliable calculations, which reproduced the experimentally observed ferromagnetism but did not explain it, were performed in the 1960s.[2]

One typically understands the paramagnetic properties of mononuclear transition metal complexes by examination of the ligand-field splitting at the metal center.[3] After having constructed the ligand-field diagram for the central metal atom, the levels are filled from the bottom with the appropriate number of electrons, in a way similar to Hund's rules for the free atom, as illustrated for a d^6 octahedral complex in Figure 1a.

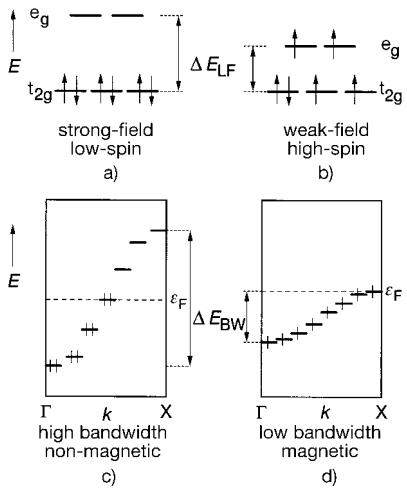

Figure 1. Schematic energy level diagrams and electron filling for a) a d^6 octahedral complex with strong-field ligands, b) the same complex with weak-field ligands, c) a one-dimensional chain with one orbital per unit cell when the bandwidth ΔE_{BW} is larger than the electron-pairing energy, d) the same chain when the bandwidth ΔE_{BW} is smaller than the electron-pairing energy. In (c) and (d) the horizontal dashed line indicates the position of the Fermi level ε_F.

[*] Prof. Dr. R. Dronskowski, Dr. G. A. Landrum
Institut für Anorganische Chemie der Technischen Hochschule
Professor-Pirlet-Strasse 1, 52074 Aachen (Germany)
Fax: (+49) 241-8888-288
E-mail: drons@hal9000.ac.rwth-aachen.de

[**] We thank Prof. Dr. Heiko Lueken and Prof. Dr. Francis J. DiSalvo for their insightful comments and the Fonds der Chemischen Industrie for their support.

In the situation sketched here (strong field, large splitting) there are no unpaired electrons and the complex will be nonmagnetic.[4] In the case of a small splitting (weak field) it may even be smaller than the energy required to pair electrons in an orbital (Figure 1b). The levels are then filled as if they were degenerate, which gives rise to the four unpaired electrons in Figure 1b. The presence of unpaired electrons leads to a paramagnetic complex. This treatment is, of course, a vast oversimplification of an approach that has been developed and refined over many years, but it conveys the essential features.

If we attempt to transfer this idea to the elemental transition metals we immediately run into difficulties. One might predict that many transition metals have unpaired electrons, so they should be magnetic. This is, of course, not the case. Only iron, cobalt, and nickel show ferromagnetic behavior (chromium and manganese exhibit antiferromagnetism, which is somewhat more complicated and will be examined separately). Metals in the second and third transition series, even those isoelectronic to the magnetic members of the first series, do not exhibit ferromagnetism. Indeed, the origins of ferromagnetism in Fe, Co, and Ni remain a matter of considerable interest (and debate) within the chemistry and physics communities.

Taking into account the paucity of magnetic metals, we find it useful to classify metals into two classes: those that are "normal" (nonferromagnetic), and those that are "anomalous" (ferromagnetic). We will first explain with this classification why practically all elemental metals are nonferromagnetic. Once that has been addressed we will explain why it is that Fe, Co, and Ni are ferromagnetic.

In the gas phase the ground-state electronic configuration of a first-row transition metal with n valence electrons is either $[Ar]4s^23d^{n-2}$ or $[Ar]4s^13d^{n-1}$. For example, in vanadium ($n=5$) the ground state is $[Ar]4s^23d^3$. Since the 3d atomic orbitals (AOs) are degenerate in the gas phase the isolated metal atom has unpaired electrons and exhibits paramagnetic behavior. When such a transition metal is embedded in a crystal, however, the 3d orbitals form bands, which simultaneously removes the fivefold degeneracy of the 3d levels and changes their occupations.

The electronic factors underlying the lack of magnetism in most elemental metal structures can be understood by using a simple model: a one-dimensional "crystal" that contains a single orbital per unit cell, namely, a chain of hydrogen atoms. If there is one electron per unit cell (or atom) there are two possible band fillings. If the band width is large—a situation analogous to the high-field ligand environment of Figure 1a—then the electrons are found paired up at the bottom of the band (Figure 1c). If, on the other hand, the band width is smaller than the energy required to pair electrons[5]—analogous to Figure 1b—then the crystal orbitals composing the band will all be half occupied (Figure 1d).

Band width is proportional to the strength of the interatomic interactions in a crystal.[6] Since these are quite strong in the elemental metals their bands are broad (ΔE_{BW} is large) and the electron filling is as shown in Figure 1c. Therefore, electrons are paired in most metals and there is no permanent magnetism. Electron fillings similar to those in Figure 1d are

  1433-7851/99/3810-1390 $ 17.50+.50/0

found for the rare-earth metals. In these elements the Fermi level usually lies within the highly contracted 4f orbitals, which are typically not involved in substantial interatomic interactions and give rise to very narrow bands. This "localized electron magnetism" in the rare-earth metals, some of which exhibit very complicated magnetic structures,[7] will not be discussed further here.

Elemental Fe, Co, and Ni exhibit "itinerant electron ferromagnetism",[7, 8, 9] that is, the conduction electrons, which are essentially delocalized, are responsible for the ferromagnetism, in contrast to the rare-earth metals (see above). Since the conduction electrons are located in bands with significant width, we can not use a picture such as that shown in Figure 1d. It is not immediately straightforward to see exactly how unpaired electrons arise in a crystal with broad bands.

Figure 2a shows a qualitative view (according to Harrison[10]) of the density of states (DOS) of a metal with significant band width. The shaded region indicates the occupied states, and its area is proportional to the total number of electrons. The DOS shown in Figure 2a includes

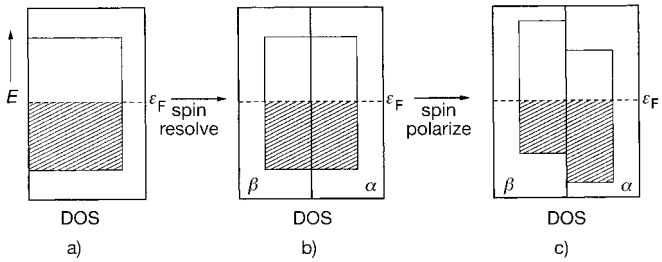

Figure 2. a) Qualitative density of states (DOS) for a metal. b) The same DOS, spin-resolved to show contributions from the α- and β-spin sublattices. c) The consequences of spin polarization upon the α- and β-spin sub-lattices. The horizontal dashed line indicates the position of the Fermi level ε_F; shaded regions indicate electron filling.

contributions from both α and β spins of these electrons.[11] If we "spin resolve" the DOS, to show the contributions from the α- and β-spin sub-lattices separately, we arrive at Figure 2b. Here the densities of states from the individual spin sub-lattices are identical; we have done nothing more than plot them individually. A magnetic moment arises when there is a difference between the occupations of the α- and β-spin sub-lattices. This difference, known as spin polarization, is illustrated in Figure 2c. Here the DOS for the β spins has moved up in energy relative to that of the α spins. Since the two densities of states must share a common Fermi level, more α than β states are populated, which gives rise to ferromagnetism.[12]

In order to understand the electronic structure of α-Fe (the body-centered cubic (bcc) phase, which is stable under standard conditions) we start with its non-spin-polarized electronic structure. While this nonmagnetic form of Fe is unstable with respect to spin polarization (α-Fe wants to be magnetic), it provides a useful starting point for the analysis.

Each iron atom in α-Fe is coordinated by eight nearest neighbors in a cubic arrangement at a distance of 2.48 Å, and another six second-nearest neighbors octahedrally arranged at 2.87 Å. This environment splits the Fe 3d orbitals into two sets at high symmetry points of the Brillouin zone (BZ): e_g (d_{z^2} and $d_{x^2-y^2}$) and t_{2g} (d_{xy}, d_{xz}, and d_{yz}) (Figure 3).

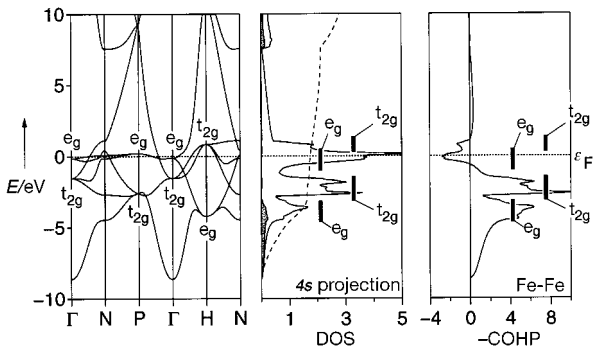

Figure 3. Non-spin-polarized band structure, DOS (shaded area: 4s projection), and Fe–Fe nearest neighbor crystal orbital Hamilton population (COHP) curve for bcc Fe. All curves are shifted so that the Fermi level ε_F, indicated with a horizontal dashed line, lies at 0 eV.

Bands at high-symmetry points in the BZ are labeled according to their symmetry, as are the major contributors to prominent peaks in the DOS and crystal orbital Hamilton population (COHP) curves (COHP is discussed in the computational methodology section below). The DOS of α-Fe exhibits a "three-peaked" shape that is typical for bcc transition metals. Surprisingly, the Fermi level ε_F lies in a region where the Fe–Fe interactions are *antibonding* (as determined from the COHP curve). The presence of antibonding levels at ε_F typically indicates structural instability; we expect these structures to undergo some form of distortion to remove or lessen the antibonding. α-Fe is no exception to this rule of thumb. However, unlike the structural distortions that are typically observed, the changes in α-Fe appear in its *electronic* structure: a realistic spin-polarized calculation results in a spin magnetic moment (difference between the occupations of the α and β spin sublattices) of 2.27 electrons, which is in excellent agreement with the experimental value of 2.21.[7] The process of spin polarization also lowers the total energy of the system by 0.426 eV. Figure 4 shows the DOS and COHP curves for spin-polarized α-Fe.

The shapes of the α DOS and the β DOS are similar and they still resemble the non-spin-polarized DOS of Figure 3, though the β spins are shifted to higher energy. Within the α-spin sub-lattice ε_F appears almost at the top of the primarily 3d

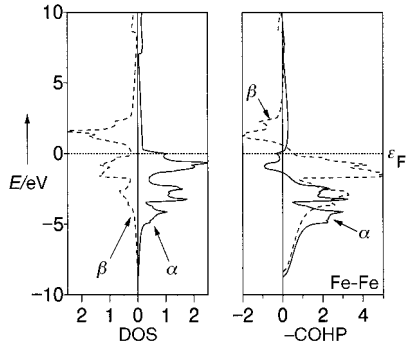

Figure 4. Spin-polarized DOS and Fe–Fe nearest neighbor COHP curves for ferromagnetic bcc Fe. In both plots the solid line corresponds to the α spins and the dashed line corresponds to the β spins. All curves are shifted so that the Fermi level ε_F, indicated with a horizontal dashed line, lies at 0 eV.

  1433-7851/99/3810-1391 $ 17.50+.50/0

states. The β spins are shifted up enough to keep the number of electrons constant. The α and β COHP curves (Figure 4) are also similar in shape (and again similar to the one in Figure 3), but their relative sizes are quite different. The α sub-lattice states that lie just below ε_F are considerably less Fe–Fe antibonding than they were before (these are the states that appeared at ε_F in Figure 3). The equivalent states in the β sub-lattice lie more than 1 eV above ε_F. The β states just below ε_F (mostly t_{2g}) are quite strongly Fe–Fe bonding, more so than the equivalent α states. Based upon the integrations of the COHP values to ε_F (ICOHPs), the Fe–Fe interactions in the β sub-lattice (ICOHP = – 0.975 eV/bond) are almost twice as bonding as those in the α sublattice (ICOHP = – 0.552 eV/bond).[13] The total Fe–Fe ICOHP (the sum of the α and β values) is – 1.527 eV/bond, more than five percent larger than that in non-spin-polarized α-Fe (– 1.448 eV/bond). *The process of spin-polarization has strengthened the Fe–Fe bonds.*

The spin-polarization process in α-Fe results in a redistribution of charge density, which is easily visualized by plotting the difference between the spin-polarized and non-spin-polarized electron densities. Figure 5 shows such contours

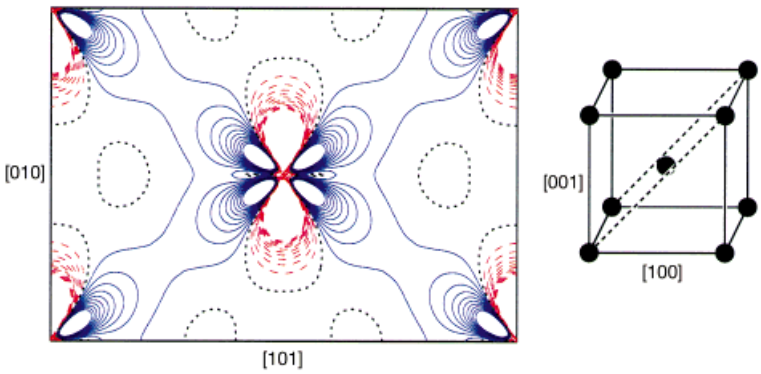

Figure 5. Contour plot of the quantity $\Delta\rho = \rho$(spin-polarized) – ρ(non-spin-polarized) evaluated in the plane delimited by the crystallographic [010] and [101] axes in α-Fe. Dashed red lines correspond to positive values, while solid blue lines correspond to negative values. Thick, dotted black lines indicate the zero contour. The location of the plane in the unit cell is illustrated schematically on the right.

evaluated in a plane through the center of the unit cell. There is a depletion of charge density in the regions of nearest-neighbor bonds (along the diagonals of the plot) and an increase in density between second-nearest-neighbor contacts along the [010] axis. Remember that in the non-spin-polarized electronic structure there are Fe–Fe antibonding states populated at ε_F. These states contribute to the electron density between nearest neighbors. Spin polarization lessens the antibonding interactions by shifting this "excess" electron density out of these regions.

We are left here with a question: Why is it that the Fe–Fe interactions in the β-spin sub-lattice are stronger than those in the α sub-lattice (Figure 4)? During spin-polarization the α states move down in energy while the β states move up. These energy shifts arise because the shielding of the nuclear charge between like spins (that is, α–α or β–β shielding) is less efficient than that between different spins (namely α–β shielding) as a consequence of the "exchange hole".[14] As spins move from the β- to the α-spin sub-lattice, the α spins experience a higher effective nuclear charge from the depletion of β spins. The opposite is true of the β spins, which experience a lower nuclear charge (are better shielded) because of the "extra" α spins. Accompanying these changes in effective nuclear charge are changes in the spatial extents of the spin sub-lattices. While the α spins become more tightly bound to the nucleus (more spatially contracted), the β spins become less tightly bound (more spatially diffuse). This explains the changes in magnitudes of the Fe–Fe COHP curves upon spin polarization: the α-spin sub-lattice is more tightly bound, more contracted, and thus Fe–Fe interactions involving the α spins are weaker. The reverse is true of the β-spin sub-lattice: it is less tightly bound, more diffuse, so Fe–Fe interactions are stronger.

If bcc iron (α-Fe) were nonferromagnetic, the Fermi level would occur in a region of Fe–Fe antibonding interactions (see Figure 3). This gives rise to an electronic structural instability that leads to spin polarization and the onset of ferromagnetism. The spin polarization results in a contraction of the α-spin sub-lattice, which shifts down in energy and gains more electrons. At the same time, the β-spin sub-lattice shifts up in energy, loses electrons, and becomes more diffuse. The net effect of these changes in the electronic structure is to remove the Fe–Fe antibonding states from the vicinity of ε_F, and increase the strength of the Fe–Fe bonds by more than five percent. The results of calculations (not shown here) upon the other ferromagnetic transition metals (Co and Ni) are similar: ε_F appears in a region of M–M antibonding in the non-spin-polarized COHP curves. This antibonding is lessened by the spin-polarization process. In the early/late nonmagnetic first row transition metals (such as vanadium or copper) ε_F lies below/above the M–M antibonding states, so there is no tendency for spin polarization, and thus magnetism, to arise. A more detailed form of this model, including an examination of antiferromagnetism within the same framework, will be presented in a forthcoming paper.

Computational Methodology

Electronic structure calculations were performed using the Linear Muffin-Tin Orbital (LMTO) method[15] within the local spin density approximation (LSDA).[16] All calculations were checked for convergence of energies, orbital moments, integrated COHP values, and magnetic moments with respect to the number of k points used in the reciprocal space integrations. The program used was TB-LMTO 4.7.[17]

While the LSDA is known to have problems with metallic Fe—and predicts a nonmagnetic face-centered cubic structure to be more stable than the magnetic bcc form[18]—it reproduces the experimental magnetic moments of Fe, Co, and Ni (2.21, 1.74, and 0.62 unpaired electrons per atom respectively[7]) quite closely (2.27, 1.60, and 0.62). The spin-polarized DOS of magnetic bcc Fe generated with a gradient correction scheme within the framework of a linear augmented plane wave (LAPW) calculation[19] is essentially identical to that generated from the LSDA within the LMTO method. Since we are not interested here in energy differences between particular structures (using instead experimental structures and lattice constants), we believe that the LSDA is accurate enough for our purposes.

Crystal orbital Hamilton population (COHP) analysis[20] is a partitioning scheme for the band structure energy (sum of the energies of the Kohn–Sham orbitals) in terms of orbital-pair contributions. COHP analysis, while in many ways analogous to the familiar crystal orbital

  1433-7851/99/3810-1392 $ 17.50+.50/0

overlap population (COOP) analysis used in extended Hückel calculations,[6, 21] provides a quantitative measure of bond strengths and is probably more appropriate for a calculation from first principles. All COHP curves are presented here in a format similar to COOP curves: positive values are bonding, and negative antibonding; this means we are plotting $-$COHP instead of COHP.

Received: September 25, 1998 [Z12453IE]
German version: *Angew. Chem.* **1999**, *111*, 1482 – 1485

Keywords: band structure calculation · electronic structure · magnetic properties · transition metals

[1] The physics community is well aware of Stoner's model that deals with ferromagnetism; unfortunately, it does not provide much insight into the bonding situation. a) W. Heisenberg, *Z. Phys.* **1928**, *49*, 619; b) E. C. Stoner, *Proc. Roy. Soc. A* **1938**, *165*, 372; c) E. C. Stoner, *Proc. Roy. Soc. A* **1939**, *169*, 339. Stoner's model included an adjustable parameter I in its original formulation; in later studies various methods to calculate I were proposed, see for example d) J. F. Janak, *Phys. Rev. B* **1977**, *16*, 255; e) O. K. Andersen, J. Madsen, U. K. Poulsen, O. Jepsen, J. Kollar, *Physica B* **1977**, *86 – 88*, 249.

[2] For example, definitive calculations of the electronic structures of Fe and Ni were made by: a) S. Wakoh, J. Yamashita, *J. Phys. Soc. Japan* **1966**, *21*, 1712; b) J. W. D. Connolly, *Phys. Rev.* **1967**, *159*, 415.

[3] a) C. J. Ballhausen, *Introduction to Ligand Field Theory*, McGraw-Hill, New York, **1962**; b) R. S. Drago, *Physical Methods in Chemistry*, Saunders College Publishing, Philadelphia, **1977**.

[4] For simplicity we neglect weak higher-order phenomena, such as temperature independent paramagnetism, which can arise in these complexes.

[5] This pairing energy includes such factors as the exchange interaction between electrons.

[6] R. Hoffmann, *Solids and Surfaces: A Chemist's View of Bonding in Extended Structures*, VCH, Weinheim, **1988**.

[7] S. Chikazumi, *Physics of Ferromagnetism*, 2nd ed., Clarendon, Oxford, **1997**.

[8] A. Aharoni, *Introduction to the Theory of Ferromagnetism*, Clarendon, Oxford, **1996**.

[9] H. Capellmann, *J. Magn. Magn. Mater.* **1982**, *28*, 250.

[10] W. A. Harrison, *Electronic Structure and the Properties of Solids. The Physics of the Chemical Bond*, Dover, New York, **1989**.

[11] The labels α and β are used to distinguish between the two possible spin orientations without making reference to any coordinate-system dependent labels such as "spin up" and "spin down".

[12] The local magnetic moments of Figure 1 d also arise as a consequence of spin polarization. In this case the narrow bands give rise to sharp peaks in the DOS. In the spin-polarized DOS of this system ε_F occurs at the top of the α DOS and the entire β DOS is found above ε_F, that is, there is no occupation of the β-spin sub-lattice.

[13] The difference in the α and β ICOHPs is a result of both the larger magnitude of the interactions in the β sub-lattice and the fact that antibonding states are populated in the α sub-lattice.

[14] H. Ibach, H. Lüth, *Solid-State Physics*, 2nd ed., Springer, Berlin, **1995**.

[15] a) O. K. Andersen, *Phys. Rev. B* **1975**, *12*, 3060; b) H. L. Skriver, *The LMTO Method*, Springer, Berlin, **1984**; c) O. K. Andersen, O. Jepsen, *Phys. Rev. Lett.* **1984**, *53*, 2571; d) O. K. Andersen, C. Arcangeli, R. W. Tank, T. Saha-Dasgupta, G. Krier, O. Jepsen, I. Dasgupta in *Tight-Binding Approach to Computational Materials Science*, No. 491, MRS, Pittsburgh, **1998**.

[16] U. von Barth, L. Hedin, *J. Phys. C* **1972**, *5*, 1629.

[17] G. Krier, O. Jepsen, A. Burkhardt, O. K. Andersen, The TB-LMTO-ASA program, version 4.7.

[18] P. Dufek, P. Blaha, K. Schwarz, *Phys. Rev. Lett.* **1995**, *75*, 3545.

[19] LAPW calculations were carried out with the program WIEN97, which is an improved and updated Unix version of the original copyrighted WIEN-code. a) P. Blaha, K. Schwarz, J. Luitz, Vienna University of Technology, **1997**; b) P. Blaha, K. Schwarz, P. Sorantin, S. B. Trickey, *Comput. Phys. Commun.* **1990**, *59*, 399.

[20] R. Dronskowski, P. E. Blöchl, *J. Phys. Chem.* **1993**, *97*, 8617.

[21] T. Hughbanks, R. Hoffmann, *J. Am. Chem. Soc.* **1983**, *105*, 3528.

Efficient Intermolecular Charge Transport in Self-Assembled Fibers of Mono- and Bithiophene Bisurea Compounds**

Franck S. Schoonbeek, Jan H. van Esch,*
Bas Wegewijs, Diederik B. A. Rep,
Matthijs P. de Haas,* Teun M. Klapwijk,
Richard M. Kellogg, and Ben L. Feringa*

Conjugated oligomers and polymers of thiophenes are among the most promising organic semiconducting molecular materials for application as thin film transistors[1] (TFT) and light-emitting diodes[2] (LED) in (opto)electronic devices. The basis for this is their highly favorable electronic properties, such as a small band gap, high charge-carrier mobility (although low compared to the mobility in some aromatic molecular crystals),[3] and high quantum yield for fluorescence.[4] The properties and performance of these materials, however, do not only depend on the electronic structure of the molecules themselves, but also critically on supramolecular features such as the molecular packing of the thiophene moieties and the morphology of thin films and crystals of those compounds.[5] Although full control of the molecular packing and morphology is still a far-fetched goal, progress has been made in directing the spacing and the orientation of π-stacked aromatic groups by making use of hydrogen bonding motifs.[6, 7] A class of compounds that is particularly well suited for the spatial organization of functional entities are (bis)urea compounds.[8] We showed recently that bisurea compounds self-assemble into ribbons, which stack into sheets or lamella.[9] The bisurea compounds have an extended conformation in the ribbons and are amenable to form multiple hydrogen bonds with neighboring molecules, and thereby provide a framework for the organization of other functional entities in ribbons and lamella (Figure 1). The

[*] Dr. J. H. van Esch, Prof. Dr. B. L. Feringa, F. S. Schoonbeek, Prof. Dr. R. M. Kellogg
Laboratory for Organic Chemistry, Stratingh Institute
University of Groningen
Nijenborgh 4, 9747 AG Groningen (The Netherlands)
Fax: (+31) 50-3634296
E-mail: esch@chem.rug.nl
feringa@chem.rug.nl

Dr. M. P. de Haas, Dr. B. Wegewijs
Radiation Chemistry Department, IRI
Delft University of Technology
Mekelweg 15, 2629 JB Delft (The Netherlands)
Fax: (+31) 15-2787421
E-mail: m.p.dehaas@iri.tudelft.nl

D. B. A. Rep, Prof. Dr. Ir. T. M. Klapwijk
Material Science Centre
University of Groningen (The Netherlands)

[**] This work was supported in part by the Netherlands Foundation for Chemical Research (SON/STW) with financial aid from the Netherlands Organization for Scientific Research (NWO). The research of Dr. J. van Esch has been made possible in part by a fellowship from the Royal Netherlands Academy of Science. The authors thank Prof. A. Brisson and J. van Breemen of the Biophysical Chemistry Department of the University of Groningen for their assistance with the electron microscopy experiments, and F. van der Horst of the department of Solid State Physics for his assistance with the electron diffraction measurements.

  1433-7851/99/3810-1393 $ 17.50+.50/0